

Development and kinematic calibration for measurement structure of a micro parallel mechanism platform

Deuk Soo Kang, Tae Won Seo and Jongwon Kim *

School of Mechanical and Aerospace Engineering, Seoul National University, Seoul, Korea

(Manuscript Received July 27, 2007; Revised January 8, 2008; Accepted January 9, 2008)

Abstract

This paper presents a micro-positioning platform based on a unique parallel mechanism developed by the authors. The platform has a meso-scale rectangular shape whose size is 20 x 23 mm. The stroke is 5 mm for both the x - and y -axes and 100 degrees for the α -axis. The platform is actuated by three sets of dual stage linear actuators: a linear motor for rough positioning and a piezo actuator for fine positioning. The developed micro-positioning platform has a measurement system that consists of three linear sensors. The position and orientation values of the movable platform can be measured directly and used in a feedback control system. Selecting 18 kinematic error parameters of a measurement system (feedback control system), a two-stage kinematic calibration method is proposed. Constant error parameters are found in the first stage and variable error parameters are found in the second stage of kinematic calibration. After kinematic calibration the position error is reduced to within $0.5 \mu\text{m}$ and error reduction rate is over 90%.

Keywords: Parallel mechanism; Kinematic analysis; Kinematic error parameter; Taguchi methodology; Kinematic calibration

1. Introduction

A parallel kinematic mechanism is a closed loop mechanism in which the end effector (mobile platform) is connected to the base by at least two independent kinematic chains. A close to infinite number of mechanisms with parallel structure can be synthesized. Many different topologies of parallel kinematic machines (PKM) have recently been studied because of the design diversity of mechanisms. The parallel kinematic machines are subdivided into planar and spatial mechanisms and are classified by the degrees-of-freedom (DOF) of the end effector and the actuator/joint arrangement [1].

A parallel mechanism can use small actuators for an end effector motion and have good dynamic characteristics because it has small inertia compared to a serial mechanism. In addition a parallel mechanism has the advantage of precision, where the length/

orientation errors are not accumulated on an end effector. A kinematic closed loop is a special feature of PKM that gives high stiffness. Meanwhile, complex control, small workspace and singularity are drawbacks of a parallel mechanism. Although a parallel mechanism has some negatives, it gives more benefits to researchers. So, many researchers, institutes and industries have studied and commercialized many different parallel structures these days.

Motion simulators, which require high speed and high acceleration, are important applications of a parallel mechanism. Machining tools for milling, turning, forming as well as soft material (plastic, wood) machining are another application. Recently, this mechanism has been widely used in robots, micro robots, positioning devices/stages, medical devices etc. The authors noticed that the parallel mechanism has these merits of small capacity actuators, good dynamic characteristics, high precision and design flexibility in the conceptual design of a novel micro-positioning platform and decided to develop an innovative parallel kinematic machine.

*Corresponding author. Tel.: +82 2 880 7138, Fax.: +82 2 875 4848
E-mail address: jongkim@snu.ac.kr
DOI 10.1007/s12206-008-0107-4

As micro/nano technologies have become widespread in various industrial fields, the machining capabilities of complex 3-D shaped micro components are required more and more in machine tools and positioning stages. To satisfy this demand, an end effector of machine tools should have high position accuracy and a large spatial work space, including high rotation capability. The dual stage system is one useful method for high position accuracy and large work space. With a dual stage system coarse actuators cover large stroke (work space) and fine actuators give high position accuracy and resolution.

Lee and Kim [2] presented an ultra-precision stage specially designed to align wafers for microlithography. The stage is composed of a global stage that provides coarse alignment motion and a micro stage that corrects positional errors in the global stage. Kwon and Cheong [3] proposed control schemes of a dual stage positioner and validated them through simulation and experiment. Takeda et al. [4] presented a parallel mechanism platform, which can achieve a large workspace and sub-micron accuracy by using dual stage systems. The proposed platform has 6 degrees of freedom but the mobility of the platform is only ± 10 degrees. These described three stages have nearly zero, or minute, rotation capability of the end effector. Therefore, complex 3-D machining can be restricted.

For complex 3-D machining, the demand for a large rotation capability as well as high position accuracy has been increased. Liu et al. [5] proposed various parallel mechanisms that have high tilting capability of the end effector and analyzed their kinematic characteristics. Oh et al. [6] performed a kinematic analysis of a micro parallel mechanism platform and designed this platform. This mechanism has over a 90° tilting capability of the end effector. Using this high tilting capability of the end effector, complex 3-D machining could be expected when this mechanism is combined with laser machining tools, for example.

This paper presents a unique parallel mechanism micro-positioning platform with dual stage system whose mobility is ± 50 degrees. This platform has a meso-scale rectangular shape whose size is 20×23 mm. The overall size of the machine is $280(w) \times 200(d) \times 408(h)$ mm, approximately desktop-sized.

The platform has 3 degrees-of-freedom (DOF): two translational motions in the x - and y -axes and a rotational motion in the α -axis (a rotation along the x -axis). The work space is 5 mm for both the x - and y -

axis and ± 50 degrees for the α -axis. The target positioning accuracy is within $0.5 \mu\text{m}$ in the x - and y -axis, respectively, and within $1.0 \mu\text{m}$ ($= 0.004$ degrees) in the α -axis on the basis of the extreme outer edge of the rotating platform.

The machine has three sets of a dual stage actuation system: a linear motor for rough positioning and a piezo actuator for fine positioning. The actuation directions of the coarse and fine actuators are vertical with each other to maximize the platform's rotation capability and resolution [6, 7].

The micro parallel mechanism platform that was developed recently has a measurement system for an end effector. Another unique characteristic of the platform is that position control is executed by this full feedback control. This measurement system, which consists of three linear sensors and directly senses the final position of the platform, can be considered another parallel mechanism. In order to achieve the high position accuracy of a machine tool, positioning stage and robot, it is important to estimate the error of its end effector due to the uncertainties in parts [8]. One method for estimating and/or eliminating the error of the end effector that comes from uncertainties in machine components is kinematic calibration. According to Hollerbach and Wampler [9] a large variety of methods have been proposed which differ according to measurement system, passive endpoint constraints and pose organization. These methods are the open loop method, closed loop method and screw axis measurement method, but the distinctions among these methods are often small and arbitrary. Koseki et al. [10] calibrated the kinematic model of parallel mechanism to improve its absolute accuracy using a laser tracking coordinate measuring system that consists of four laser stations and a wide angle retro-reflector. Patel and Ehmann [11] used redundant legs for calibration. The distances between an end effector and a point of base frame are calculated by using redundant legs, and these data are utilized in calibration. Zhuang [12] performed the self calibration of a Stewart platform by installing the proper number of redundant sensors in proper locations and creating a suitable measurement residual by exploring conflicting information provided by redundant sensing.

For accurate measurement of position and precise control, a two-stage kinematic calibration for this measurement system is performed. The values of kinematic parameters are found from kinematic cali-

bration and these parameters are embodied in a control algorithm. After calibration, position errors and orientation errors are reduced to less than $0.5 \mu\text{m}$ and 0.003 degrees, respectively.

The paper is organized as follows. In Section 2, a kinematic analysis of the parallel mechanism is presented. Section 3 describes the main design features of the real micro positioning platform that has been assembled. In Section 4 and 5, kinematic calibration for the micro-positioning platform will be presented. Finally, some concluding remarks follow in Section 6.

2. Kinematic analysis of the parallel mechanism

The research objective is the development of a micro-positioning platform that could be used in micro machining of a complex 3-D shape. To achieve this objective, the high tilting capability of the micro-positioning platform and a high positing accuracy are required. In addition, having a small-sized machine is more advantageous in respect to energy saving, space, maintenance, etc.

The micro-positioning platform is based on a new spatial 3-DOF parallel mechanism, which has the distinct advantage of high mobility. The 3-DOF parallel mechanism consists of a base plate, a movable platform, and three legs that connect the base plate and the movable platform. Each leg is connected to the actuator combination of coarse and fine actuators.

A kinematics model of the manipulator is shown in Fig. 1. The first and second legs have identical chains, each of which consists of a link connected to the movable platform by a universal joint, and to the base plate by a passive revolute joint. The third leg has a different chain, which consists of a planar four-bar parallelogram connected to the movable platform and the base plate by universal joints.

The combination of three legs leaves the mechanism with two translational DOF in the O - xy plane

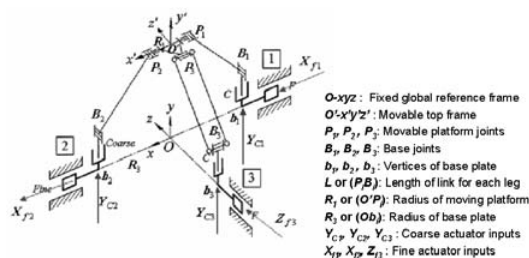


Fig. 1. A parallel mechanism of the micro-positioning platform.

and one rotational DOF along the x -axis.

The kinematic constraint of the mechanism is that the length of each link is constant as shown in Eq. (1).

$$|P_i - B_i| = L, \quad \text{where} \quad i = 1, 2, 3 \quad (1)$$

Three scalar equations can be generated from Eq. (1) for the three links, as follows:

$$(x - R_1 + R_3 - X_{f1})^2 + (y - Y_{c1})^2 = L^2 \quad (2)$$

$$(x + R_1 - R_3 - X_{f2})^2 + (y - Y_{c2})^2 = L^2 \quad (3)$$

$$x^2 + (-R_1 \cos \alpha + R_3 - Z_{f3})^2 + (R_1 \sin \alpha - Y_{c3})^2 = L^2 \quad (4)$$

Forward kinematics obtain the position (x, y) and α from the value of each actuator. In these equations, there are three values of the end effector and six values of the actuator.

Backward kinematics obtain the six values of each actuator from the three values of the end effector. A problem arises when solving the backward kinematics of the mechanism, since six unknown values of actuator exist while only three constraint equations are available. By fixing three values of actuator, all six unknown values are determined.

Design parameters are optimized through the geometric model of the solution space (GMSS). Design parameters are non-dimensionalized and are embodied in a finite solution space. Objective function is plotted in GMSS and constraints are considered. The optimal design parameters are determined through this procedure.

The workspace analysis is performed based on the backward and forward kinematics. The stroke in the x -axis is ± 2.5 mm and that in the y -axis is from 0 to 5 mm. This satisfies the 5×5 mm workspace. In any point of (x, y) of this workspace, the tilting angle in the α -axis satisfies a 100-degree requirement. The minimum and maximum tilting angles in this workspace are 112 and 139 degrees, respectively.

Singularity analysis is also performed. It is found that no singularity exists in the workspace.

3. Micro-positioning platform

The micro-positioning platform is designed and assembled. An overview of this platform is shown in Fig. 2. The whole size of the machine including the measurement system for full feedback control is $280(\text{w}) \times 200(\text{d}) \times 408(\text{h})$ mm. Each link has a unique

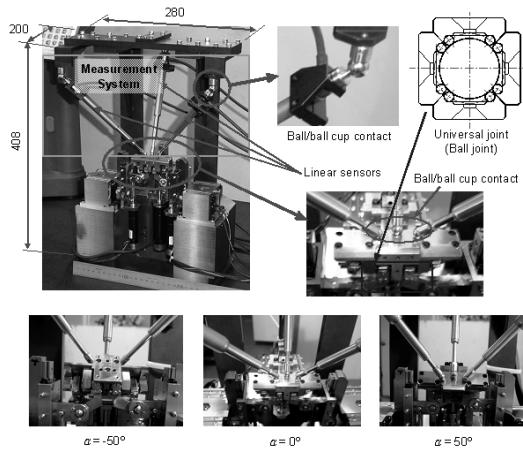


Fig. 2. Photo of the micro-positioning parallel mechanism platform.

ball joint, which is shown in the upper right corner of Fig. 2. This ball joint has two independent rotational axes with low friction. Also in Fig. 2, three linear sensors are seen attached to the movable platform. Since the three linear sensors directly sense the final position of the platform, full feedback control is possible. At the bottom of Fig. 2, three photos show the high tilting capability of the movable platform. Each photo shows the tilting posture of the platform at -50, 0 and 50 degrees, respectively.

The micro-positioning platform can be used in laser machining. While the micro-positioning platform traces the machining path, a one-dimensional movement of the laser source determines the machining depth [13]. The characteristics and cutter path generation algorithm for laser machining were investigated by some of the authors.

4. Kinematic calibration

4.1 Design and kinematic analysis of measurement system

The developed micro-positioning platform can be divided into two parts. One is the actuation system which consists of three sets of a coarse actuator and a fine actuator. The other part is a measurement system, which senses the position and orientation of an end effector (movable platform) and submits these measured values into a full feedback control algorithm. The measurement system is composed of three linear sensors. From this full feedback control system, high position accuracy of the movable platform can be

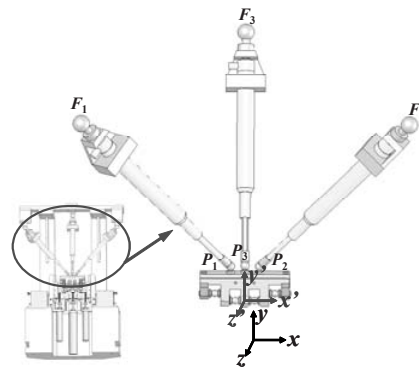


Fig. 3. Measurement system and its coordinate system.

obtained.

The measurement system of micro-positioning platform consists of three linear sensors as described above and the configuration of this system is shown in Fig. 3. Two translation (x - and y -direction) and one rotation (α -direction) sets of data are obtained from three reading values of linear sensors. The measurement system can be considered a parallel mechanism because the upper fixed frame, three linear sensors and movable platform make closed loop chains. This parallel mechanism looks like a simpler parallel mechanism than an actuation mechanism, so kinematic analysis of this system can be easily and efficiently conducted. Kinematic analysis of this measurement system is described as in the following.

The length data of the linear sensor are obtained from backward kinematics. The relation between the position of the movable platform and the length data of the linear sensor is as Eq. (5).

$$L_i = |P_i - F_i| \quad \text{where } i = 1, 2, 3 \quad (5)$$

The values F_i are fixed values but the position values P_i are varied according to the translational and/or rotational motion of the movable platform. The position values relative to global coordinate system are obtained from Eq. (6). Eq. (7) represents rotation matrix of the movable platform which has angle of α about the x -axis.

$$P_i = R \cdot {}^M P_i + P_C \quad (6)$$

$$R = \begin{bmatrix} 1 & 0 & 0 \\ 0 & \cos \alpha & -\sin \alpha \\ 0 & \sin \alpha & \cos \alpha \end{bmatrix} \quad (7)$$

Here P_i and ${}^M P_i$ are position vectors relative to the global coordinate (x - y - z coordinate) and local coordinate (x' - y' - z' coordinate). In initial posture of the movable platform, the local coordinate coincides with the global coordinate. The $P_C = (x, y, 0)$ vector is the movement of the movable platform. Matrix R is a rotation matrix about the x -axis of this coordinate system.

The position and rotation data are obtained from linear sensor reading values using forward kinematics. The position and rotation values of the movable platform are calculated numerically from Eq. (8) below. The scalar form of Eq. (8) is presented as Eq. (9).

$$[P_i - F_i]^T [P_i - F_i] = L_i^2 \tag{8}$$

$$\begin{aligned} & \left({}^M P_{ix} + x - F_{ix} \right)^2 + \left({}^M P_{iy} \cos \alpha - {}^M P_{iz} \sin \alpha + y - F_{iy} \right)^2 \\ & + \left({}^M P_{iy} \sin \alpha + {}^M P_{iz} \cos \alpha - F_{iz} \right)^2 - L_i^2 = 0 \end{aligned} \tag{9}$$

4.2 Kinematic error parameter of measurement system and sensitivity analysis

Eighteen Kinematic error parameters are chosen in the kinematic calibration and Fig. 4 shows these error parameters. There are six kinematic error parameters in the upper frame of the measurement system: three position error parameters ($\Delta f_x, \Delta f_y, \Delta f_z$) and three length error parameters of triangle ($\Delta r_{11f}, \Delta r_{12f}, \Delta r_{2f}$) which has vertexes like F_1, F_2 and F_3 . There are nine kinematic error parameters on the movable platform. They are position error parameters ($\Delta p_x, \Delta p_y, \Delta p_z$), orientation error parameters ($\Delta \varepsilon_x, \Delta \varepsilon_y, \Delta \varepsilon_z$) and three length error parameters of a small triangle on a movable platform. The other three error parameters ($\Delta L_1, \Delta L_2, \Delta L_3$) are kinematic error parameters of the length of linear sensors.

Taguchi methodology is known as the most useful method for ‘Design of Experiments’ [14]. This method can be used in sensitive analysis when its input and output are properly modified. Sensitive kinematic error parameters are selected by using Taguchi methodology in this paper. For efficiency and high precision, finding sensitive error parameters is important. To find sensitive kinematic error parameters, simulation is performed before kinematic calibration.

$L_{81} (3^{40})$ orthogonal array and three levels are selected for sensitivity simulation of 18 kinematic error parameters [15]. Dynamic characteristics system analysis of the Taguchi methodology is used for this

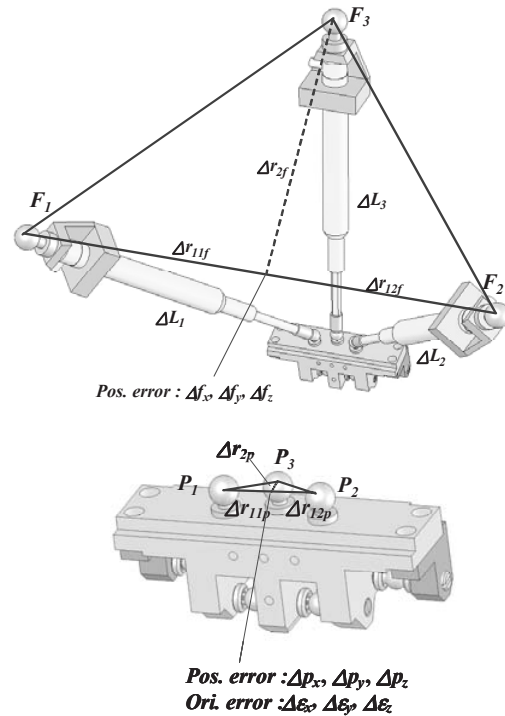


Fig. 4. Kinematic error parameters of measurement system.

sensitivity analysis. Input data are true values of position (and orientation) and output data are calculated position (orientation), where kinematic error parameters are included in simulation. In this simulation 18 error parameters are treated as controllable variables. Three levels of kinematic error parameters are used in simulation. Level 1 has a $-5 \mu\text{m}$ error deviation from nominal kinematic parameters such as $f_x, p_x, \varepsilon_x, L_x$. Kinematic error parameters which are related to orientation angle have -0.0212 degrees (a $-5 \mu\text{m}$ error deviation in the extreme outer surface of the movable platform). Level 2 has a $0 \mu\text{m}$ error deviation; level 3 has a $5 \mu\text{m}$ error deviation from nominal kinematic parameters. Nominal values of each kinematic parameter are measured values. The values where error deviation is added to the nominal kinematic parameter are used in the simulation.

Twenty-one points are selected for this simulation in forward and backward x - (y -)directions and 33 points are selected in forward and backward α -directions, respectively. For α -directional simulation, the simulation regions are divided into three regions because of restrictions of the test equipment. Each region has a 4-degree range and these regions exist around $-45, 0, 45$ degrees’ orientation. Table 1 shows

Table 1. Test points for kinematic calibration test and simulation.

No.	x (mm)	y (mm)	No.	α (deg.)	α (deg.)	α (deg.)
1	-2.50	0	1	-47.00	-2.00	43.00
2	-2.25	0.25	2	-46.60	-1.60	43.40
3	-2.00	0.50	3	-46.20	-1.20	43.80
4	-1.75	0.75	4	-45.80	-0.80	44.20
...
18	1.75	4.25	8	-44.20	0.80	45.80
19	2.00	4.50	9	-43.80	1.20	46.20
20	2.25	4.75	10	-43.40	1.60	46.60
21	2.50	5.00	11	-43.00	2.00	47.00

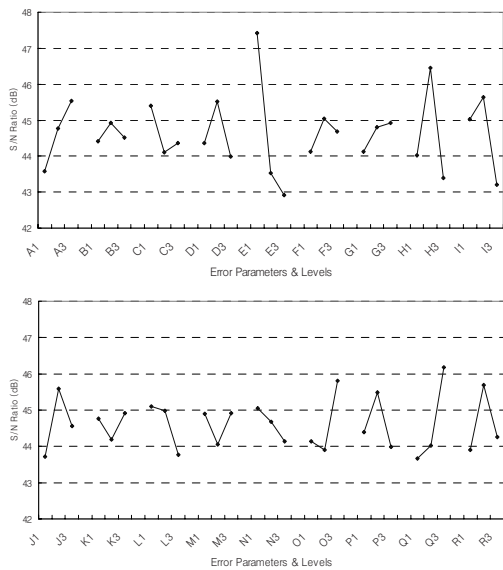


Fig. 5. Signal to Noise ratio response graphs due to 18 error parameters.

test points for kinematic calibration.

From this Taguchi methodology Signal to Noise ratios are calculated. It is known that the larger the variation of S/N ratio between levels, the more sensitive are the parameters. The S/N ratio can be calculated from Eq. (10).

$$S/N(\eta) = -10 \log_{10}(MSD) \tag{10}$$

$$MSD = (y_1^2 + y_2^2 + \dots) / n$$

Where, y_1, y_2, \dots = Results of experiments, observations or quality characteristics

m = Target value of results

n = Number of repetitions (y_i)

The simulation results of Signal to Noise Ratio response are shown in Fig. 5. In this graph, the variables A to R mean $\Delta \varepsilon_x$ (A), $\Delta \varepsilon_x$ (B), $\Delta \varepsilon_x$ (C), Δr_{11p} (D), Δr_{12p} (E), Δr_{2p} (F), Δp_x (G), Δp_y (H), Δp_z (I), Δr_{11f} (J), Δr_{12f} (K), Δr_{2f} (L), Δf_x (M), Δf_y (N), Δf_z (O), ΔL_1 (P), ΔL_2 (Q), ΔL_3 (R). Numbers 1, 2 and 3 are the levels of each parameter.

From this S/N ratio analysis, three kinematic error parameters of Δr_{12p} (E in Fig. 5), ΔL_2 (Q in Fig. 5) and $\Delta \varepsilon_x$ (A in Fig. 5) can be considered as sensitive parameters.

4.3 Kinematic calibration of measurement system

The measurement system of the micro-positioning parallel mechanism platform is calibrated to achieve high accuracy (the measurement system is shown in Figs. 2 and 3). Manufacturing and assembling errors for the micro-positioning platform are compensated by this kinematic calibration. Kinematic calibration consists of ‘identification of error parameters’, ‘error modeling’, ‘measurement’, ‘parameter selection through calibration algorithm’ and ‘controller model modification considering selected error parameters’.

High precision two-stage kinematic calibration is presented in this paper. In two-stage kinematic calibration, constant kinematic error parameters are calculated and variable kinematic error parameters are adopted in the second stage. As described above, three kinematic error parameters Δr_{12p} , ΔL_2 and $\Delta \varepsilon_x$ are more sensitive than other parameters. ΔL_2 is a sensitive error parameter and the ball and ball cup joint of the linear sensor can have micro-range slip according to the position and orientation of the movable platform. Three linear sensor error parameters ΔL_1 , ΔL_2 , ΔL_3 also have geometric constraints with each other, so mathematical representation exists between these parameters. For these reasons kinematic error parameters ΔL_1 , ΔL_2 , ΔL_3 are treated as three variable kinematic error parameters.

In this paper a two-stage kinematic calibration method is proposed as mentioned above. Fifteen kinematic error parameters that satisfy Eq. (11) are found in first stage calibration. In Eq. (11) subscripts t and m mean true value and measured values of translation and orientation, respectively.

$$\text{Minimize } (x_t - x_m)^2 + (y_t - y_m)^2 + (\alpha_t - \alpha_m)^2 \tag{11}$$

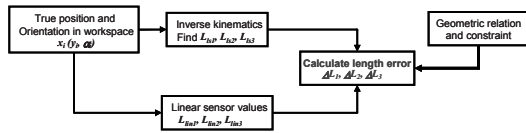


Fig. 6. Calculation procedure of variable error parameters ΔL_i .

After invariable kinematic error parameters are found, the variable error parameters are measured from test points which are summarized in Table 1. Variable error parameters ΔL_1 , ΔL_2 , ΔL_3 should satisfy Eq. (12). In this equation L_{i_ls} and L_{i_lm} mean true values of linear sensor length measured by the laser displacement sensor and reading values of the linear sensor, respectively.

$$\text{Minimize } (L_{i_ls} + \Delta L_i - L_{i_lm})^2 \text{ where } i=1, 2, 3 \quad (12)$$

There are geometric constraints or Eq. (13) between three error parameters according to its movement direction. The values ΔL_i are found from these relationships (Eq. 12 and 13) in the workspace along each direction. From measured ΔL_i and linear interpolation between test points, the variable kinematic error parameters ΔL_i are found in the whole work space.

$$\begin{aligned} x\text{-direction} : \Delta L_1 &= -\Delta L_2 & \Delta L_3 &\approx 0 \\ y\text{-direction} : 1.347 \cdot \Delta L_1 &= 1.347 \cdot \Delta L_2 = \Delta L_3 \\ \alpha\text{-direction} : \Delta L_1 &= \Delta L_2 \end{aligned} \quad (13)$$

The calculation procedure of variable error parameter ΔL_i is shown in Fig. 6. Variable error parameters are found following procedure at test points.

5. Kinematic calibration test

5.1 Test equipment

The test rig for calibration is shown in Fig. 7. This test rig is composed of four laser displacement sensors, reflection plates, attachment jig and micro stages for distance adjustment between laser sensors and reflection plates.

There are 21 test points for translational direction and 33 ($=3 \times 11$) for rotational direction as described in Table 1. A translation test is performed covering all the workspace in one setup of the test rig, but the measurement range of displacement sensors does not cover all the tilting angles in the rotation test. Thus the workspace is divided into three small regions (-45,

Table 2. Comparison of error values between before and after calibration.

Test direction	Maximum error value		
	Before calibration ($\mu\text{m}, \times 10^{-3}\text{deg.}$)	After calibration ($\mu\text{m}, \times 10^{-3}\text{deg.}$)	Error red. Rate (%)
x forward	2.96	0.12	95.95
x backward	10.25	0.27	97.37
y forward	7.44	0.25	96.64
y backward	7.43	0.48	93.54
α forward	86.8	1.8	97.93
α backward	93.9	2.8	97.02

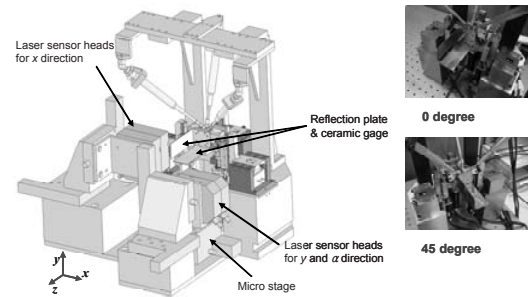


Fig. 7. 3-D model of test rig for kinematic calibration test and the photos of rotation test equipment.

0 and 45-degree regions) to test large tilting angles of the movable platform. The test directions are forward x -, y -, α -directions and backward x -, y -, α -directions.

5.2 Test results

From the calibration test, constant and variable kinematic error parameters are obtained. Modifying the kinematic analysis module of the full feedback control algorithm, a verification test for kinematic calibration is performed.

Table 2 shows the error reduction between before- and after-kinematic calibration. The error reduction rate ranges from 93.54 to 97.93%. The translation and rotation errors are over $10 \mu\text{m}$ and 0.09 degrees before kinematic calibration. After two-stage kinematic calibration, the translational error values are reduced to below than $0.5 \mu\text{m}$ and rotational error is below than 0.003 degrees.

Fig. 8 shows the error reduction result of position and rotation over work space of the micro-positioning platform when two-stage kinematic calibration is

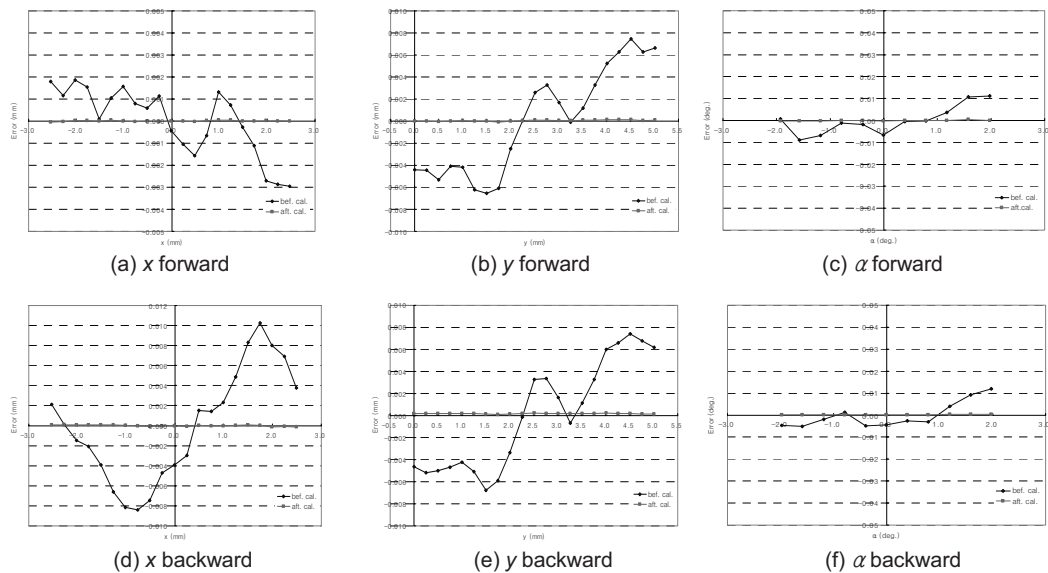


Fig. 8. Position and rotation error reduction by applying kinematic calibration.

applied.

6. Conclusions

A three-degree of freedom parallel mechanism micro-positioning platform with a 100-degree tilting capability has been presented. It is controlled by a dual-stage controller. The two unique features of the dual-stage controller are that the actuation directions of the coarse and fine actuators are in vertical with each other and that it has a full feedback control loop. A two-stage kinematic calibration study of the measurement system is also proposed. Constant error parameters are found in the first stage, and three variable error parameters are found in the second stage of kinematic calibration. The position error values of the micro-positioning platform are reduced to within 0.5 μm and the orientation error values are reduced to below 0.003 degrees. The error reduction rate ranged from 93.54 to 97.93%.

A dual servo control algorithm for the more precise and rapid movement is now being studied. The laser machining process, which is combined with this micro-positioning platform, is also being studied as future work.

Acknowledgment

This paper was sponsored by the Brain Korea 21

Program and partly by the Micro-thermal System ERC.

References

- [1] M. Weck and D. Staimer, Parallel kinematic machine tools – current state and future potentials, *CIRP Annals* 51 (2002) 671-683.
- [2] C. W. Lee and S. W. Kim, An ultraprecision stage for alignment of wafers in advanced microlithography, *Precision Engineering* 21 (1997) 113-122.
- [3] S. J. Kwon and J. Cheong, Robust minimum-time control with coarse/fine dual-stage mechanism, *Journal of Mechanical Science and Technology* 20 (11) (2006) 1834-1847.
- [4] Y. Takeda, K. Ichikawa, H. Funabashi and K. Hirose, An in-parallel actuated manipulator with redundant actuators for gross and fine motions, Proceedings of the 2003 IEEE, Taipei, Taiwan. (2003) 749-754.
- [5] X.-J. Liu, J. Wang and G. Pritschow, A new family of spatial 3-DoF fully-parallel manipulators with high rotational capability, *Mechanism and Machine Theory* 40 (2005) 475-494.
- [6] K.-K. Oh, X.-J. Liu, D. S. Kang and J. Kim, Optimal design of a micro parallel positioning platform Part I: Kinematic analysis, *Robotica* 22 (2004) 599-609.
- [7] K.-K. Oh, X.-J. Liu, D. S. Kang and J. Kim, Opti-

- mal design of a micro parallel positioning platform Part II: Real machine design, *Robotica* 23 (2005) 109-122.
- [8] S. R. Lim, K. Kang, S. Park, W. C. Choi, J.-B. Song, D. Hong and J. K. Shim, Error analysis of a parallel mechanism considering link stiffness and joint clearances, *Journal of Mechanical Science and Technology* 16 (6) (2002) 799-809.
- [9] J. M. Hollerbach and C. W. Wampler, The calibration index and taxonomy for robot kinematic calibration methods, *International Journal of Robotics Research* 15 (1996) 573-591.
- [10] Y. Koseki, T. Arai, K. Sugimoto, T. Takatiji and M. Goto, Design and accuracy evaluation of high-speed and high precision parallel mechanism, IEEE Proceedings of International Conference on Robotics and automation, Leuven, Belgium. (1998) 1340-1345.
- [11] A. J. Patel and K. F. Ehmann, Calibration of a hexapod machine tool using a redundant leg, *International Journal of Machine Tools & Manufacture* 40 (2000) 489-512.
- [12] H. Zhuang, Self-calibration of parallel mechanisms with a case study on Stewart platforms, *IEEE Transactions on Robotics and Automation* 13 (3) (1997) 387-397.
- [13] C. S. Ahn, T. W. Seo, J. Kim and T. W. Kim, High-tilt parallel positioning mechanism development and cutter path simulation for laser micro-machining, *Computer-Aided Design* 39 (2007) 218-228.
- [14] K. Lee and J. Kim, Controller gain tuning of a simultaneous multi-axis PID control system using the Taguchi method, *Control Engineering Practice* 8 (2000) 949-958.
- [15] G. S. Peace, Taguchi Methods, Addison-Wesley Publishing Company, Reading, Massachusetts, USA, (1994).